Multi-species dynamical density functional theory

Multi-species dynamical density functional theory

B. D. Goddard, A. Nold, and S. Kalliadasis

Citation: J. Chem. Phys. **138**, 144904 (2013); doi: 10.1063/1.4800109
View online: http://dx.doi.org/10.1063/1.4800109
View Table of Contents: http://jcp.aip.org/resource/1/JCPSA6/v138/i14
Published by the American Institute of Physics.

Multi-species dynamical density functional theory

B. D. Goddard,[a] A. Nold, and S. Kalliadasis[b]
Department of Chemical Engineering, Imperial College London, London SW7 2AZ, United Kingdom

(Received 16 January 2013; accepted 22 March 2013; published online 12 April 2013)

We study the dynamics of a multi-species colloidal fluid in the full position-momentum phase space. We include both inertia and hydrodynamic interactions, which strongly influence the non-equilibrium properties of the system. Under minimal assumptions, we derive a dynamical density functional theory (DDFT), and, using an efficient numerical scheme based on spectral methods for integro-differential equations, demonstrate its excellent agreement with the full underlying Langevin equations. We utilise the DDFT formalism to elucidate the crucial effects of hydrodynamic interactions in multi-species systems. © *2013 AIP Publishing LLC*. [http://dx.doi.org/10.1063/1.4800109]

I. INTRODUCTION

We consider the dynamics of colloidal fluids, where mesoscopic particles (of typical size 1 nm–1 μm) are suspended in a bath of many more, much smaller, and much lighter particles. In such systems, interest lies in the dynamics on a wide range of lengthscales from the size of the particles to the macroscale.[1] Hence, due to the multiscale nature of the problem, standard continuum models such as the Navier-Stokes equation are unsuitable. The alternative is reduced models which correctly capture the full range of both microscopic and macroscopic dynamics, obtained by using elements from the statistical mechanics of liquids.

Of particular interest here are systems containing multiple species of colloidal particles. Typical examples include biological systems such as blood flow, where there are multiple types of cells, possibly along with artificially introduced species such as nanoparticles used in drug delivery, or microfluidic devices with differently shaped, sized, or charged colloidal particles. These examples are linked to recent advances in biophysics[2] and microfluidics[3–5] which in turn have led to a growing interest in the behaviour of multi-species colloidal systems. Such systems also lead to rich dynamics such as phase separation, frustrated crystallization,[6] and, as we will see later, complicated indirect inter-species interactions.

Their full dynamics are described by the deterministic Newton's equations for the positions and momenta of both the colloidal and bath particles. However, due to the large number of particles involved in the corresponding physical systems, this leads to very high-dimensional problems which are computationally intractable. One way in which to reduce the dimension is to use the intrinsic timescales of the systems. Due to their much smaller masses, the bath particles typically have much higher velocities than the colloidal particles. Hence, for timescales significantly larger than the typical time between collisions of the bath particles (around 10^{-15} s), one may average out the rapid fluctuations of the bath particles, leading to a coarse-grained stochastic (Langevin) description containing only the positions and momenta of the colloidal particles.

In such a model, it is necessary to include the interactions of the bath and colloidal particles. These take two forms: (a) the random collisions of the bath particles with the colloidal particles, and (b) the forces on the colloidal particles due to flows induced in the bath by their motion, known as hydrodynamic interactions (HI). Figure 1 depicts an example of these induced flows. Whilst HI include crucial physics, their inclusion complicate the numerical implementation of the Langevin dynamics. For example, for N particles and a standard timestepping algorithm, including HI (rather than a simple self-friction term) transforms the problem from $\mathcal{O}(N)$ to order $\mathcal{O}(N^3)$ at each timestep. Due to this high computational cost, especially for physically relevant numbers of particles, we require a reduced model which captures the multiscale dynamics of the problem.

One such class of reduced models are dynamical density functional theories (DDFTs), a number of which have been developed. A DDFT is a statistical mechanical approach which aims to reduce the full dynamics to closed equations for the dynamics of the one-body position distribution. For a single species of colloidal particle, a typical DDFT is a continuity equation for the density $\rho(\mathbf{r}, t)$, with $\mathbf{r}$ a single position coordinate, i.e., $\partial_t \rho(\mathbf{r}, t) + \nabla_{\mathbf{r}} \cdot \mathbf{J}([\rho], \mathbf{r}, t) = 0$, where $\mathbf{J}$, a functional of ρ, remains to be determined. The main computational benefit of a DDFT is that the dimension is fixed at the physical dimension of the system (plus one time dimension), independently of the number of particles.

Although it has been shown rigorously that such DDFTs exist,[7] the functional form of $\mathbf{J}$ is unknown. In contrast, for practical implementations, this functional, or a good approximation to it, needs to be given explicitly. Due to the widespread success of equilibrium density functional theory (DFT) for classical fluids (see, e.g., the pioneering works in Refs. 8 and 9 and more recent reviews in Refs. 10 and 11), this functional is usually based on the free energy of a related equilibrium system. This approach also ensures that the DDFT agrees with the static DFT at equilibrium.

Most existing DDFTs neglect either the momenta of the colloidal particles,[12] or the HI,[13–18] or both, as in the

[a]b.goddard@imperial.ac.uk
[b]s.kalliadasis@imperial.ac.uk

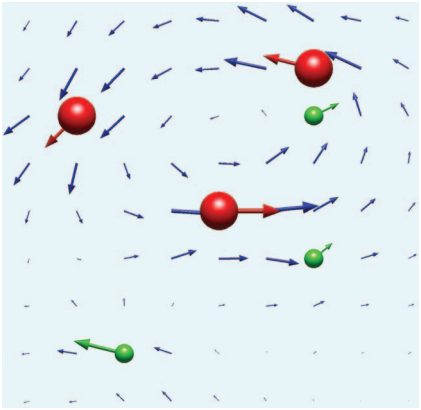

FIG. 1. A schematic of the flows induced in the bath (blue arrows) by the motion of two differently sized species of colloidal particles (red and green spheres/arrows).

pioneering work of Marconi and Tarazona.[19] In recent work,[20,21] we have systematically derived and implemented an accurate and efficient DDFT which includes all of these effects for one species of colloidal particle. In this work, we extend our DDFT formalism to multiple species, demonstrating the very good agreement with the full underlying stochastic dynamics, as well as the importance of both HI and inertia in multi-species systems. Examples of physical systems in which HI and inertia are expected to play crucial roles are wetting phenomena[22–24] (and confined systems in general), aerosol deposition and cloud formation,[25–29] and the transport of colloidal particles in oscillatory flows such as in the cardiovascular system and oscillatory flow mixing.[30] In contrast, previous work on multi-species DDFT[31–34] has utilised the most basic DDFT in which both inertia and HI are neglected and as such it is unclear that existing approaches are sufficiently accurate to describe problems such as the above.

The manuscript is laid out as follows. In Sec. II we outline our DDFT formalism for multiple particle species, including both inertia and HI. In Sec. III we describe the numerical validation of our DDFT and demonstrate the crucial influence of HI. Finally, in Sec. IV we summarize our results and discuss some open problems and future work.

II. DDFT FORMALISM

Consider a system containing ν species of colloidal particles suspended in a bath of many more, much smaller, and much lighter particles. As discussed in the Introduction, these species may differ in a wide range of physical properties. Here we treat the masses of the particles directly and encapsulate all other properties via an external potential for each species (which may differ, for example, if an electric field is applied to species with different charges) and interparticle potentials (which again may differ in both intra- and inter-species interactions).

For systems with a fixed number N_α particles of each species $\alpha = 1, \dots \nu$, we are interested in the positions $\mathbf{r}_{\alpha,i}$ and momenta $\mathbf{p}_{\alpha,i}$ of the colloidal particles (where $\mathbf{r}_{\alpha,i}$ ($\mathbf{p}_{\alpha,i}$) is position (momentum) of the ith particle of species α). From now on we consider timescales significantly larger than the typical collision time of bath particles, but smaller than the typical timescale on which the colloidal particles move a distance the order of their size. As such, we may consider a bath of constant temperature, which interacts with the colloidal particles through two terms in the Langevin equations. For ease of notation we define the total number of particles $N = \sum_{\alpha=1}^{\nu} N_\alpha$ and construct length $3N$ vectors $\mathbf{r}^N = (\mathbf{r}_{\alpha,i})$ and $\mathbf{p}^N = (\mathbf{p}_{\alpha,i})$ of all colloidal particle positions and momenta. We then have

$$\begin{aligned} \frac{\mathrm{d}\mathbf{r}^N}{\mathrm{d}t} &= \mathbf{M}^{-1}\mathbf{p}^N, \\ \frac{\mathrm{d}\mathbf{p}^N}{\mathrm{d}t} &= -\nabla_{\mathbf{r}^N} V(\mathbf{r}^N, t) - \mathbf{\Gamma}(\mathbf{r}^N)\mathbf{p}^N + \mathbf{A}(\mathbf{r}^N)\mathbf{f}^N(t). \end{aligned} \tag{1}$$

Here $\mathbf{M}$ is the diagonal mass matrix and V is the potential, which we will generally consider as the sum of an external potential and two-body inter-particle potentials. The effects of the bath are modelled by two terms. First, the motion of the colloidal particles causes flows in the bath, which in turn cause forces on the colloidal particles. The coupling between the momenta of the colloidal particles and their resulting forces, already referred to as HI, is described by the $3N \times 3N$ positive definite friction tensor $\mathbf{\Gamma}$. Second, the random collisions of the bath particles with the colloidal particles are modelled by the final stochastic term where the strength of the noise is related to $\mathbf{\Gamma}$ via a generalized fluctuation-dissipation theorem $\mathbf{A} = \sqrt{k_B T \mathbf{M}\mathbf{\Gamma}}$, where the square root exists as $k_B T \mathbf{M}\mathbf{\Gamma}$ is positive definite.[35] Here T is the (constant) temperature and k_B is Boltzmann's constant. The random forces are given by mean zero, uncorrelated Gaussian white noise such that $\mathbf{f}^N = (f_k(t))$ with $\langle f_k(t)\rangle = 0$ and $\langle f_k(t) f_\ell(t')\rangle = 2\delta_{k,\ell}\delta(t-t')$.

The friction tensor $\mathbf{\Gamma}$ may be decomposed into 3×3 blocks ($\mathbf{\Gamma} = (\mathbf{\Gamma}_{\alpha,i;\beta,j})$) with $\mathbf{\Gamma}_{\alpha,i;\beta,j}(\mathbf{r}^N) = \delta_{\alpha,\beta}\delta_{i,j}\gamma_\alpha \mathbf{1} + \tilde{\mathbf{\Gamma}}_{\alpha,i;\beta,j}(\mathbf{r}^N)$. Here, $\mathbf{1}$ is the 3×3 identity matrix determining the (diagonal) self-friction term for each particle and the terms $\tilde{\mathbf{\Gamma}}_{\alpha,i;\beta,j}(\mathbf{r}^N)$ contain all the HI. The fluctuation dissipation theorem ensures that the HI have no influence at equilibrium. However, they are typically long-range (decaying only as the inverse of particle separations) and are vital in correctly describing the dynamic behaviour of many systems.

After averaging over the noise and initial particle distribution, the Langevin equations can be rewritten as a Fokker-Planck equation, which is a $(6N+1)$-dimensional partial differential equation (PDE) for the evolution of the N-body distribution function $f^{(N)}(\mathbf{r}^N, \mathbf{p}^N, t)$. As such, for large numbers of particles the only computationally tractable approach requires Monte-Carlo methods, which are of the same complexity as solving the Langevin equations. As mentioned, in the presence of HI, these scale as N^3 (due to requiring the square root of $\mathbf{\Gamma}$), which prevents direct simulation for even moderate numbers of particles.

In order to obtain a computationally tractable reduced model, we turn to statistical mechanics. Analogously to the Runge-Gross theorem for quantum systems,[36] Chan and Finken[7] showed (for a one-species system) the existence of a DDFT for the time evolution of the one-body density $\rho(\mathbf{r}_1, t) = N \int \mathrm{d}\mathbf{r}_1' \mathrm{d}\mathbf{p}^N f^{(N)}(\mathbf{r}^N, \mathbf{p}^N, t)$, where $\mathrm{d}\mathbf{r}_1'$ indicates integration over all positions except $\mathbf{r}_1$. The obvious extension to multi-species systems is to determine a DDFT for

the one-body densities $\rho_\alpha(\mathbf{r}_{\alpha,1},t)=N\int \mathrm{d}\mathbf{r}'_{\alpha,1}\mathrm{d}\mathbf{p}^N f^{(N)}(\mathbf{r}^N,\mathbf{p}^N,t)$, $\alpha=1,\dots\nu$. However, while the existence of such DDFTs shows that all information in the full N-body distribution is contained in the one-body densities, the proof is non-constructive and it remains to determine a multi-species DDFT of the form $\partial_t\rho_\alpha(\mathbf{r}_{\alpha,1})=-\nabla_{\mathbf{r}_{\alpha,1}}\cdot\mathbf{J}_\alpha(\mathbf{r}_{\alpha,1},t,[\{\rho_\beta\}])$. That is, it remains to determine the functional form of the currents $\mathbf{J}_\alpha$, which depend on the one-body densities of all species.

Recently, we have derived a general DDFT containing both inertia and HI[20,21] for a single species of colloidal particle. We now outline the extension of the derivation to an arbitrary number of species (see our earlier work[21] for details). The overall strategy is to take momentum moments of the Fokker-Planck equation, which leads to an infinite hierarchy of equations which must be closed to obtain a computational scheme. Here, as previously,[21] we choose to truncate at the momentum level (analogous to the Navier-Stokes equation). The issue is then that, for N-body potentials or HI, these equations still contain the full N-body distribution and we require an approximate closure scheme which we then verify numerically.

The first of these approximations, known as the adiabatic approximation, is common to all DDFTs and was originally suggested by Marconi and Tarazona.[19] This approximates the non-equilibrium Helmholtz free energy by the corresponding functional for an equilibrium system with the same one-body densities. Although this is an uncontrolled approximation, it has a number of advantages. First, it ensures that the DDFT equilibrates to the static DFT solution. Second, whilst the exact form of the Helmholtz free energy is not known explicitly, various approximations such as fundamental measure theory[37–39] for hard spheres and mean field theory for densely packed soft particles[40] have been used successfully for a wide range of equilibrium systems.

The second approximation is that the one-body distributions, $f^{(1)}_\alpha(\mathbf{r}_{\alpha,1},\mathbf{p}_{\alpha,1},t)=N\int \mathrm{d}\mathbf{r}'_{\alpha,1}\mathrm{d}\mathbf{p}'_{\alpha,1}f^{(N)}(\mathbf{r}^N,\mathbf{p}^N,t)$, $\alpha=1,\dots\nu$, are at local equilibrium. That is, we take

$$f^{(1)}_\alpha(\mathbf{r}_{\alpha,1},\mathbf{p}_{\alpha,1},t)=\frac{\rho_\alpha(\mathbf{r}_{\alpha,1},t)}{(2\pi m_\alpha k_BT)^{3/2}}\times\exp\left(-\frac{|\mathbf{p}_{\alpha,1}-m_\alpha\mathbf{v}_\alpha(\mathbf{r}_{\alpha,1},t)|^2}{2m_\alpha k_BT}\right),$$

where $\mathbf{v}_\alpha(\mathbf{r}_{\alpha,1},t)$ is the local velocity for species α. Although this approximation is also uncontrolled, it is widely used in the literature.[41] In our recent study in Ref. 21, we have discussed the new effects and difficulties introduced by going beyond this approximation.

The third approximation, which is included for ease of presentation and is straightforward to generalize, is that the HI tensors are two-body:

$$\tilde{\mathbf{\Gamma}}_{\alpha,i;\beta,j}(\mathbf{r}^N)=\delta_{\alpha,\beta}\delta_{ij}\sum_{(\kappa,\ell)\neq(\alpha,i)}\mathbf{Z}^{(1)}_{\alpha,\kappa}(\mathbf{r}_{\alpha,i},\mathbf{r}_{\kappa,\ell})+(1-\delta_{\alpha,\beta}\delta_{ij})\mathbf{Z}^{(2)}_{\alpha,\beta}(\mathbf{r}_{\alpha,i},\mathbf{r}_{\beta,j}).$$

We note that there exists a two-body expansion for the full friction tensor for hard spheres of different sizes at arbitrary separations.[42] To close the two-body HI term, we also assume that we may write the two-body distributions as

$$f^{(2)}_{\alpha,\beta}(\mathbf{r}_\alpha,\mathbf{p}_\alpha,\mathbf{r}_\beta,\mathbf{p}_\beta,t)=f^{(1)}_\alpha(\mathbf{r}_\alpha,\mathbf{p}_\alpha,t)f^{(1)}_\beta(\mathbf{r}_\beta,\mathbf{p}_\beta,t)\times g_{\alpha,\beta}(\mathbf{r}_\alpha,\mathbf{r}_\beta,[\{\rho_\kappa\}]),$$

for some known correlation functionals $g_{\alpha,\beta}$. Such an approximation is standard[43,44] and can be justified through a maximum entropy closure.[44] In addition, although we assume that these correlation functionals introduce no explicit momentum correlation (the corresponding equation with $g_{\alpha,\beta}(\mathbf{r}_\alpha,\mathbf{r}_\beta,\mathbf{p}_\alpha,\mathbf{p}_\beta,[\{\rho_\kappa\}])$ is known to hold), as described previously,[21] this does not prevent the resulting DDFT from capturing non-local velocity correlations. Since this approximation neglects terms of the same order in $\mathbf{p}$ as the local equilibrium approximation, we expect these two approximations to be valid in similar regimes.

These assumptions lead to a DDFT which consists of a continuity equation for the density of each species,

$$\partial_t\rho_\alpha(\mathbf{r})=-\nabla_\mathbf{r}\cdot\big(\rho_\alpha(\mathbf{r})\mathbf{v}_\alpha(\mathbf{r})\big),\tag{2}$$

and an evolution equation for the velocity of each species,

$$\begin{aligned}&\partial_t\mathbf{v}_\alpha(\mathbf{r})+(\mathbf{v}_\alpha(\mathbf{r},t)\cdot\nabla_\mathbf{r})\mathbf{v}_\alpha(\mathbf{r},t)\\&\quad=-\frac{1}{m_\alpha}\nabla_\mathbf{r}\frac{\delta\mathcal{F}[\{\rho_\beta\}]}{\delta\rho_\alpha}-\gamma_\alpha\mathbf{v}_\alpha(\mathbf{r},t)\\&\qquad-\sum_{\beta=1}^{\nu}\int\mathrm{d}\tilde{\mathbf{r}}\rho_\beta(\tilde{\mathbf{r}},t)g_{\alpha,\beta}(\mathbf{r},\tilde{\mathbf{r}},[\{\rho_\kappa\}])\\&\qquad\times\left[\mathbf{Z}^{(1)}_{\alpha,\beta}(\mathbf{r},\tilde{\mathbf{r}})\mathbf{v}_\alpha(\mathbf{r},t)+\mathbf{Z}^{(2)}_{\alpha,\beta}(\mathbf{r},\tilde{\mathbf{r}})\mathbf{v}_\beta(\tilde{\mathbf{r}},t)\right],\end{aligned}\tag{3}$$

where $\mathcal{F}$ is the (equilibrium) Helmholtz free energy.

This equation shows that the material derivative of the velocity is given by a pressure-like term that depends on the Helmholtz free energy functional, a standard friction term, and two non-local terms that depend on the HI. The first of these, involving $\mathbf{Z}^{(1)}_{\alpha,\beta}$, combines with the standard friction term to give a density-dependent effective friction. The second, involving $\mathbf{Z}^{(2)}_{\alpha,\beta}$, non-locally couples the velocities of all species.

As for the one-species case,[21] neglecting the HI terms reduces this general DDFT to the multiple-species analogue of the DDFT derived by Archer:[13] $\partial_t\mathbf{v}_\alpha(\mathbf{r})+(\mathbf{v}_\alpha(\mathbf{r},t)\cdot\nabla_\mathbf{r})\mathbf{v}_\alpha(\mathbf{r},t)=-\frac{1}{m_\alpha}\nabla_\mathbf{r}\frac{\delta\mathcal{F}[\{\rho_\beta\}]}{\delta\rho_\alpha}-\gamma_\alpha\mathbf{v}_\alpha(\mathbf{r},t)$. If, along with neglecting these terms, we consider the overdamped (high-friction) limit, the terms on the left-hand side are negligible and inserting the resulting expression for $\mathbf{v}_\alpha$ into the continuity equation gives the standard overdamped DDFT,

$$\partial_t\rho_\alpha(\mathbf{r})=\frac{\gamma_\alpha}{m_\alpha}\nabla_\mathbf{r}\cdot\left(\rho_\alpha(\mathbf{r})\nabla_\mathbf{r}\frac{\delta\mathcal{F}[\{\rho_\beta\}]}{\delta\rho_\alpha}\right),$$

as used in previous work on multi-species DDFT.[31–34] This passage to the high friction or overdamped regime can be made rigorous (at least in the one-species case),[45] but it is important to note that in the case of a non-trivial friction tensor, the rigorous derivation leads to a different definition of the diffusion tensor than in the standard DDFT[12] obtained from the Smoluchowski equation.

III. NUMERICAL VERIFICATION AND EXPERIMENTS

In this section we will first validate the DDFT (2) and (3) against the full underlying Langevin dynamics (1). This is necessary as the derivation of the DDFT requires a number of uncontrolled approximations. Second, we will demonstrate an efficient numerical implementation of our DDFT for systems with an arbitrary number of particles, in particular, the effects of HI in a multi-species system.

We now summarize our choice of Helmholtz free energy for the DDFT and HI for both the DDFT and Langevin dynamics. The Helmholtz free energy has the form,

$$\mathcal{F}[\{\rho_\kappa\}] = k_B T \sum_{\alpha=1}^{\nu} \int \mathrm{d}\mathbf{r}_\alpha \rho_\alpha(\mathbf{r}_\alpha, t)\big(\ln(\Lambda_\alpha^3 \rho_\alpha(\mathbf{r}_\alpha, t)) - 1\big) + \sum_{\alpha=1}^{\nu} \int \mathrm{d}\mathbf{r}_\alpha V_\alpha^{(1)}(\mathbf{r}_\alpha, t)\rho_\alpha(\mathbf{r}_\alpha, t) + \mathcal{F}_{\mathrm{exc}}[\{\rho_\kappa\}],$$

where the first two terms correspond to a mixture of ν ideal gases with de Broglie wavelengths λ_α (which turn out to be irrelevant) subject to external potentials $V_\alpha^{(1)}$. The final term, called the excess over ideal gas free energy is generally unknown.

We first consider hard sphere systems for which we use Rosenfeld's fundamental measure theory (FMT)[37,39] approximation to $\mathcal{F}_{\mathrm{exc}}[\{\rho_\alpha\}]$. This defines a number N_w of explicit, geometrically derived weights w_a^α and an explicit function Φ, which give

$$\mathcal{F}_{\mathrm{exc}}[\{\rho_\kappa\}] = k_B T \sum_{a=1}^{N_w} \int \mathrm{d}\tilde{\mathbf{r}} \Phi(\{n_a(\tilde{\mathbf{r}})\}) \quad \text{with}$$

$$n_a(\mathbf{r}) = \sum_{\alpha=1}^{\nu} \int \mathrm{d}\tilde{\mathbf{r}} \rho_\alpha(\tilde{\mathbf{r}}) w_a^\alpha(\mathbf{r} - \tilde{\mathbf{r}}).$$

Note that the FMT formalism can treat mixtures of hard spheres of different sizes, but we will concentrate on mixtures of spheres with the same diameter but with different responses to an external potential.

In modelling the HI, we take different approaches for the DDFT and Langevin dynamics. In the DDFT we take the 11-term two-body expansion of Jeffrey and Onishi.[42] We note that this is expected to be accurate for widely separated particles and that it may be extended to include lubrication effects which become important when particles are not well separated. For the Langevin dynamics we require that $\mathbf{\Gamma}$ is positive definite (both physically, so that the system is dissipative, and numerically, so that $\sqrt{\mathbf{\Gamma}}$ exists). As arbitrary truncations of the two-body expansion are not necessarily positive-definite, we choose $\mathbf{\Gamma} = k_B T \mathbf{M}^{-1} \mathbf{D}^{-1}$, where $\mathbf{D}$ is the (positive-definite) Rotne-Prager diffusion tensor[46] $\mathbf{D} = (\mathbf{D}_{ij})$ with

$$\mathbf{D}_{ij}(\mathbf{r}^N) = \gamma^{-1} \left[\delta_{ij}\mathbf{1} + \delta_{ij} \sum_{\ell \neq i}^{N} \mathbf{D}_{11}(\mathbf{r}_i - \mathbf{r}_\ell) + (1 - \delta_{ij})\mathbf{D}_{12}(\mathbf{r}_i - \mathbf{r}_j) \right]. \tag{4}$$

We expect these two approximations to agree for systems in which the particles are on average well separated. However, irrespective of the other approximations in the DDFT, we should not expect exact agreement, but rather qualitative agreement and an understanding and elucidation of the effects of HI.

Here, and in the corresponding two-body expansion we introduce a hydrodynamic diameter $\sigma_{\mathrm{H}} < \sigma$ increasing the accuracy of the two-body approximation. Such an effective diameter is appropriate for many commonly studied colloidal particles which consist of a hard core with a layer of polymer[6] and has been used in previous DDFTs with HI.[12,20,21] We will choose $\sigma_{\mathrm{H}} = 0.5\sigma$, but good agreement was found between the DDFTs and stochastic calculations containing HI for $\sigma_{\mathrm{H}} \lesssim 0.75$. Our choice for the diffusion tensor is therefore

$$\mathbf{D}_{12}(\mathbf{r}) = \frac{3}{8}\left(\frac{\sigma_{\mathrm{H}}}{|\mathbf{r}|}\right)\left[\mathbf{1} + \frac{\mathbf{r}\otimes\mathbf{r}}{|\mathbf{r}|^2}\right] + \frac{1}{16}\left(\frac{\sigma_{\mathrm{H}}}{|\mathbf{r}|}\right)^3\left[\mathbf{1} - 3\frac{\mathbf{r}\otimes\mathbf{r}}{|\mathbf{r}|^2}\right] \tag{5}$$

and $\mathbf{D}_{11} = \mathcal{O}(1/r^4)$, which is negligible for diffuse systems. As stated previously, in this work we consider systems in which all species of hard particles have the same diameter (and also the same σ_{H}). However, the two-body expansion used in the DDFT was originally formulated for differently-sized spheres,[42] and thus the method is straightforward to generalize. One further requirement when including HI is the determination of the correlation functional $g_{\alpha,\beta}$ in (3). Whilst it is theoretically possible to determine g as a functional derivative of the free energy through the Ornstein-Zernike relation,[8] as in the one-species case, we find it sufficient to use the most basic hard sphere excluded volume approximation, $g(\mathbf{r}, \tilde{\mathbf{r}}) = 1$ for $|\mathbf{r} - \tilde{\mathbf{r}}| > 1$ and zero elsewhere. The main advantage of such an approximation is that, although not entirely consistent with FMT, it significantly reduces the computational complexity of the problem with little loss of accuracy.

We solve the Langevin dynamics using a standard Euler-Maruyama time-stepping routine,[47] where the hard-sphere interparticle potential is slightly softened to produce a differentiable potential $V_2(|\mathbf{r}_1 - \mathbf{r}_2|) = |\mathbf{r}_1 - \mathbf{r}_2|^{-48} - |\mathbf{r}_1 - \mathbf{r}_2|^{-24} + 1/4$ for $|\mathbf{r}_1 - \mathbf{r}_2| < 2^{1/24}$ and zero otherwise. The time step is chosen such that halving it produces no appreciable difference in the dynamics. The initial condition is found by slice-sampling[48] the (unnormalized) equilibrium N-body distribution.

In order to reduce the complexity of the DDFT computations, we consider systems in which the external potentials are spherically symmetric, i.e., $V_\alpha^{(1)}(\mathbf{r}) = V_\alpha^{(1)}(r)$. This reduces the full three-dimensional densities and velocities to one-dimensional functions of only the radial distance, i.e., $\rho_\alpha(\mathbf{r}) = \rho_\alpha(r)$ and $\mathbf{v}_\alpha(\mathbf{r}) = \mathbf{v}_\alpha(r)$. We use one-dimensional Chebyshev spectral methods[49] appropriately extended to integro-differential equations[22] and a Runge-Kutta solver.[50] Such methods are exponentially convergent and require few grid points, typically around 100 for the systems presented here. We obtain the initial condition via the simultaneous solution of the Euler-Lagrange equations for each species, $\frac{\delta \mathcal{F}[\{\rho_\beta\}]}{\delta \rho_\alpha} - \mu_\alpha = 0$. In order to increase the efficiency of the numerical scheme, we rewrite the DDFT for $y_\alpha = \log \rho_\alpha$

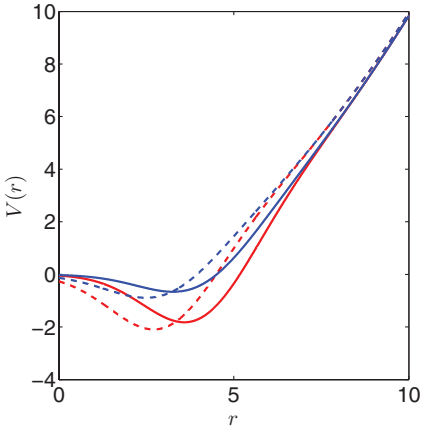

FIG. 2. External potentials for the two species (red and blue lines, respectively) at $t = 0$ (solid lines) and $t > 0$ (dashed lines).

$+ V_\alpha^{(1)}$ with $y_\alpha(\infty) = 0$, which captures the exponential decay of the system. We also treat the singularity in the divergence at the origin by mirroring the solution and solving on $(-\infty, \infty)$ rather than on $[0, \infty)$.

We have previously[20,21] validated a range of DDFTs for single species colloidal particle against the underlying stochastic dynamics, and have also demonstrated the effects of including inertia and HI. We shall demonstrate the agreement between the DDFT (2) and (3) and the Langevin dynamics (1) to be similarly very good for multiple species of particles. We first consider a system with two species, which differ in their response to the external potential. From now on we will set σ_α, m_α, and k_BT to unity, which define the units of length, time, and energy. We define an external potential for each species by $V_\alpha^{(1)}(r; r_0) = V_0(1 - h)r^2 - Z_\alpha \exp[-(r - r_0)^2/4]$, where $h(r, r_0) = [\mathrm{erf}((r + r_0)/4) - \mathrm{erf}((r - r_0)/4)]/2$ is a smooth cutoff function. Here the external potentials for the two species depend only upon the values of Z_α. For our first example, we take $N_1 = N_2 = 25$, $\gamma = 2$, $V_0 = 0.1$, $r_0 = 4$ for $t = 0$, $r_0 = 3$ for $t > 0$, $Z_1 = 2.5$, and $Z_2 = 1.25$. These potentials are shown in Fig. 2. We note here that the precise choice of these parameters is unimportant; equally good results were obtained for a wide range of parameters and other forms of external potentials.

In Fig. 3, we show snapshots of the radial particle distributions (number of particles in an infinitesimal shell at radius r, given by $4\pi r^2 \rho(r)$) and velocities for both the DDFT and Langevin calculations. As can be seen, the agreement is very good. We note here that the DDFT calculations typically take around 10 s on a standard desktop computer, compared to around 10^5 s for the Langevin simulations. Whilst the effects of HI are visible in the velocity plots, and also in the mean positions and velocities in Fig. 4, they are not large. However, this system contains a relatively small number of particles. We now move on to consider a system with ten times as many particles, setting $N_1 = N_2 = 250$, $\gamma = 2$, $V_0 = 0.03$, $r_0 = 10$ for $t = 0$, $r_0 = 5$ for $t > 0$, $Z_1 = 1.5$, and $Z_2 = 0.75$. These parameters ensure that the maximum density of particles is approximately the same as in the previous example. As can be seen in Fig. 5, the inclusion of HI now leads to qualitatively different dynamics, emphasising the importance of such effects in systems with macroscopic numbers of particles.

We now consider an example in which the effect of HI is crucial in understanding the dynamics of the system. We again consider two species, but now exert very different external

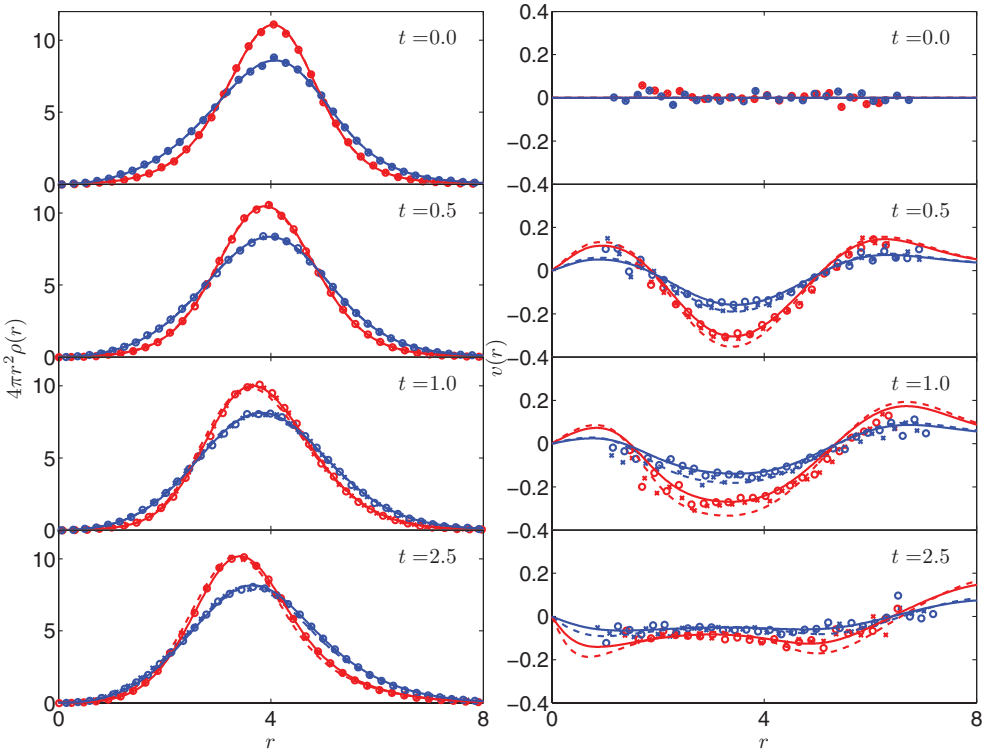

FIG. 3. Snapshots of radial particle distributions and velocities at various times for 25 particles of each species. Species 1 in red, species 2 in blue. Lines show DDFT calculations, symbols Langevin simulations for systems both with (solid/circles) and without (dashed/crosses) HI.

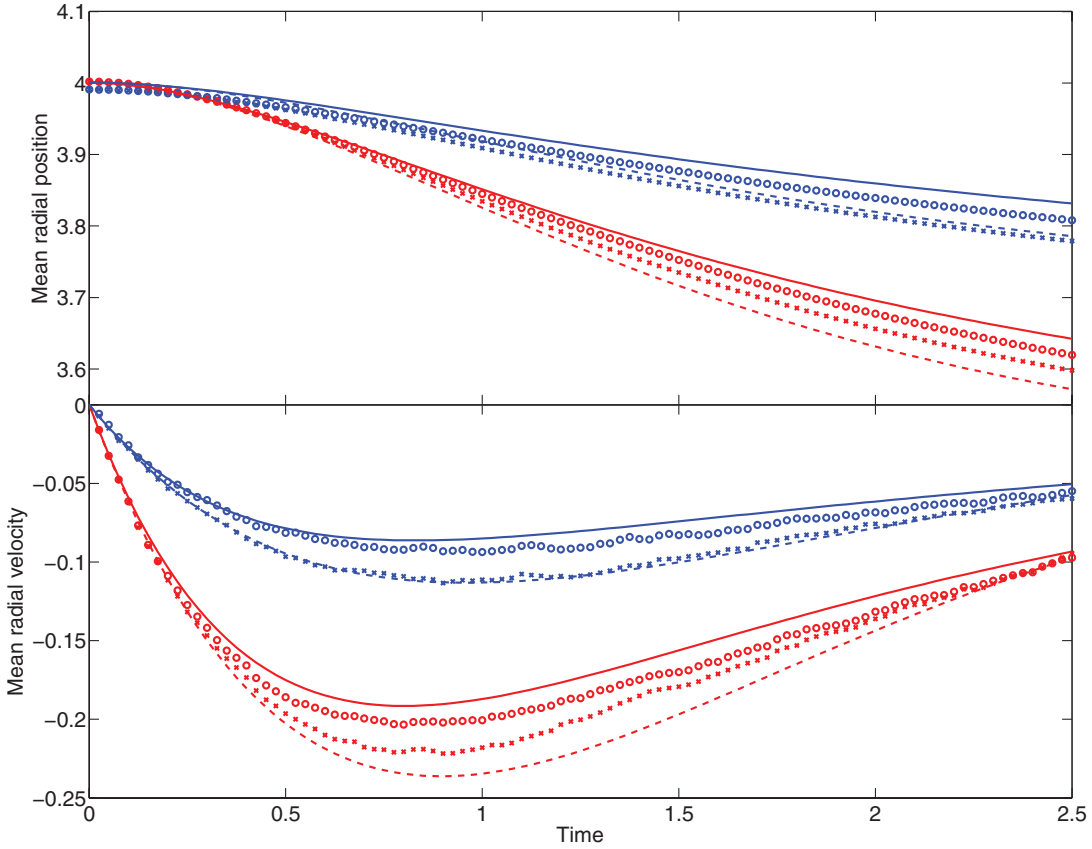

FIG. 4. Mean radial positions and velocities for 25 particles of each species; lines and symbols as in Fig. 3.

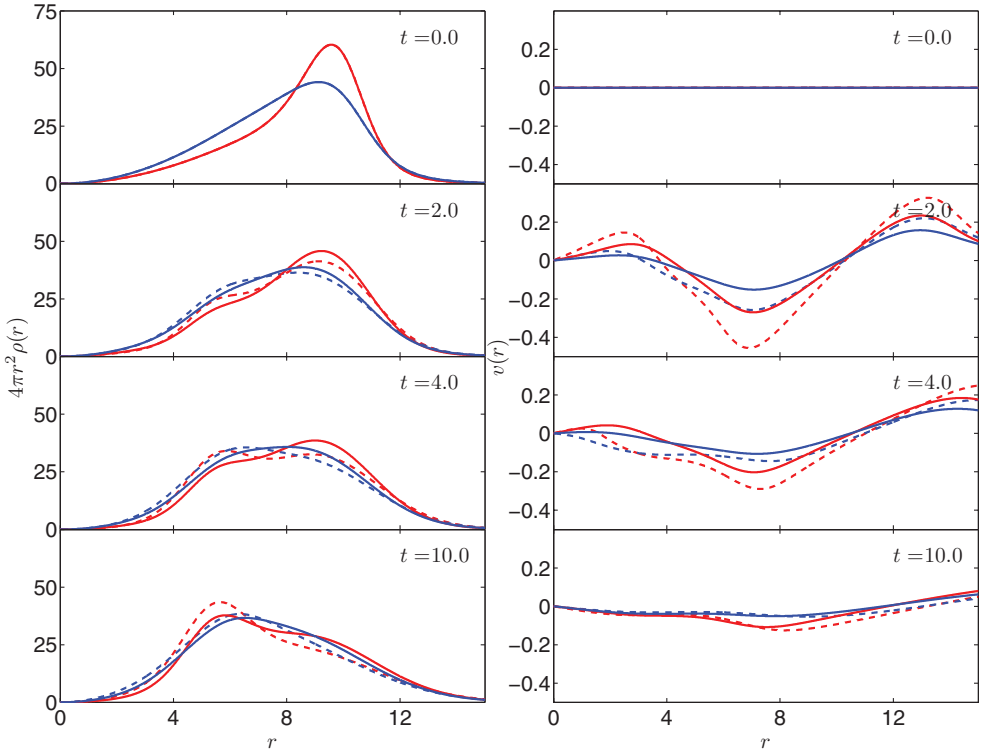

FIG. 5. Snapshots of radial particle distributions and velocities at various times for 250 particles of each species. Lines as in Fig. 3.

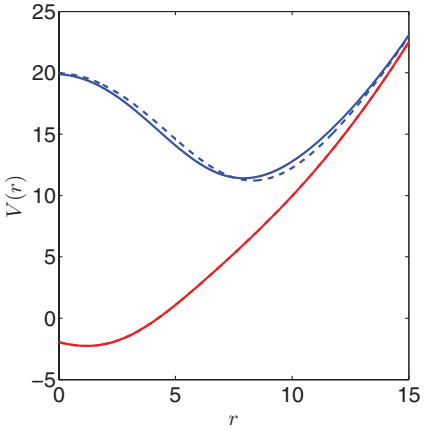

FIG. 6. External potentials (6) for species 1 (red line) and (7) for species 2 (blue lines; solid for $r_2(t) = 7$, dashed for $r_2(t) = 8$).

potentials on each species:

$$V_1^{(1)} = -0.25\exp(-(r - r_1(t))^2/16), \tag{6}$$

$$V_2^{(1)} = -0.25\exp(-(r - r_2(t))^2/16) + 20\exp(-r^2/64), \tag{7}$$

where $r_1(t) = 2$ and $r_2(t)$ is either 7 for $t = 0$ and 8 for $t > 0$, or vice versa. These potentials are shown in Fig. 6. The first term in each potential localises the particles around $r_i(t)$, whilst the second term for the second species excludes those particles from a region around the origin, effectively separating the two species so there are no direct interactions. We fix $N_2 = 10$ and will vary N_1. A typical equilibrium configuration with $N_1 = 150$ is shown in Fig. 7, along with the equilibrium particle distributions.

In Fig. 8 we show the mean radial velocity of species 2 for varying N_1. It is clear that if HI are neglected, the dynamics (red, dashed lines) are essentially independent of N_1, which is due to the lack of direct interactions. However, when including HI, there is a strong dependence on N_1; as N_1 increases the dynamics become more strongly damped. That is, the HI due to the presence of the first species inhibit the movement of the second species, in much the same way as would be expected by the presence of a wall. Hence, we find that the inclusion of the non-local HI terms is essential in determining the correct physics of such systems. In addition, the monotonic behaviour of the mean velocity of species 2 suggests that it should be possible to measure properties of small numbers of particles of one species to determine properties (such as the number of particles) of another species, even if there is no direct interaction.

As an additional example of the effectiveness of our multi-species DDFT, we consider a case that demonstrates size-mediated phase separation. In this case we use a mean-field approximation to the excess free energy $\mathcal{F}_{\text{exc}}[\{\rho_\alpha\}]$. In particular, we choose, for a pairwise inter-particle potential $V^{(2)}$,

$$\mathcal{F}_{\text{exc}}[\{\rho_\alpha\}] = \frac{1}{2}\sum_{\alpha,\beta=1}^{\nu}\int \mathrm{d}\mathbf{r}_\alpha \mathrm{d}\mathbf{r}_\beta \rho_\alpha(\mathbf{r}_\alpha)\rho_\beta(\mathbf{r}_\beta)V^{(2)}(\mathbf{r}_\alpha, \mathbf{r}_\beta).$$

This approximation is expected to be accurate for soft particles at high densities. For the interparticle potential we choose a Gaussian repulsion between particles of species α and β, $V^{(2)}_{\alpha,\beta}(\mathbf{r}_\alpha, \mathbf{r}_\beta) = 0.5\exp(-|\mathbf{r}_\alpha - \mathbf{r}_\beta|^2/a^2_{\alpha,\beta})$, where $a_{1,1} = 0.2$, $a_{2,2} = 1$, and $a_{1,2} = a_{2,1} = (a_{1,1} + a_{12})/2 = 0.6$. This models two species of soft particles of different diameters, with species 1 smaller than species 2.

The two species are subject to the same external potential, given by

$$V^{(1)}(r, t) = \begin{cases} 0.01r^2 - 10\exp(-r^2/80) & \text{for } t = 0 \\ 0.01r^2 - 10\exp(-r^2/16) & \text{for } t > 0. \end{cases}$$

We consider a system with 25 particles of each species and $\gamma = 2$. As shown in Fig. 9, this changes from a weakly confining potential to a more strongly confining one, resulting in a phase separation with the smaller particles preferentially located nearer the origin. For the case of soft particles, there is no standard method of including HI, and we instead choose to neglect these effects and concentrate on the difference between the inertial and overdamped DDFTs. As can be seen in Fig. 10, there is very good agreement between both DDFTs

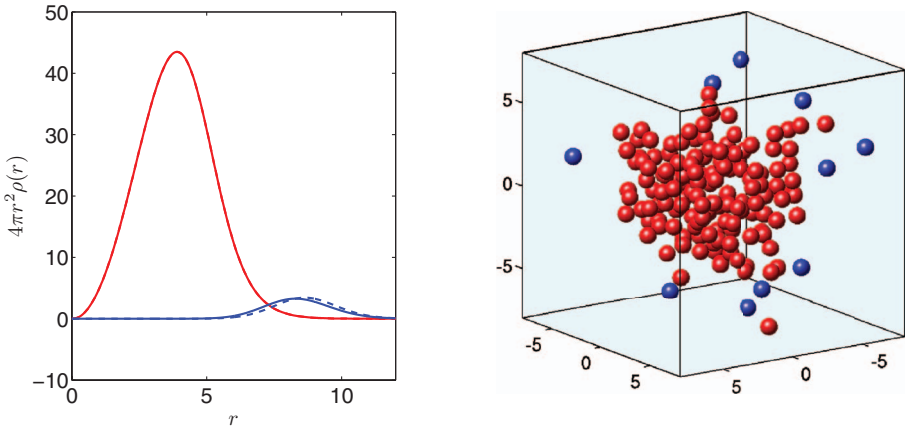

FIG. 7. Left plot shows the equilibrium particle distributions for $N_1 = 150$ particles of species 1 in red and $N_2 = 10$ particles of species 2 in blue. Solid lines correspond to $r_2 = 7$ and dashed lines to $r_2 = 8$. Note that the curves for species 1 are indistinguishable. Right plot shows a typical equilibrium configuration for the same system. We show only the case $r_2 = 7$; the case for $r_2 = 8$ is similar and differences between particular realizations are uninformative.

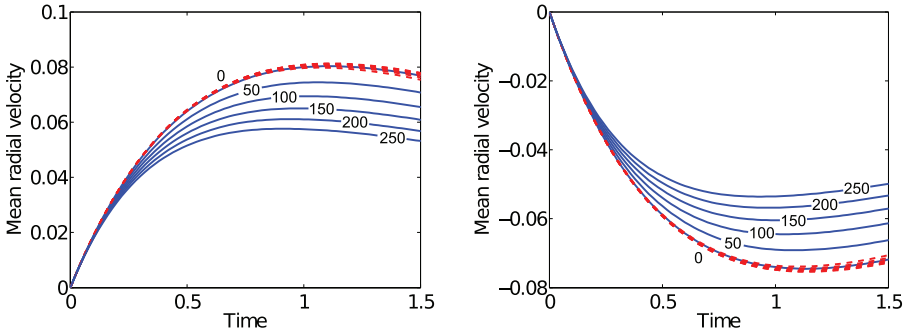

FIG. 8. Mean radial velocity for the 10 particles of species 2 as a function of time for various number of particles N_1 of species 1. Left plot shows the system with $r_2(0) = 7$ and $r_2(t > 0) = 8$, right plot shows the system with $r_2(0) = 8$ and $r_2(t > 0) = 7$. Red dashed lines show the DDFT neglecting HI, the results of which are essentially independent of N_1 due to the lack of direct interactions between the systems. Blue lines include HI and show a strong dependence on N_1.

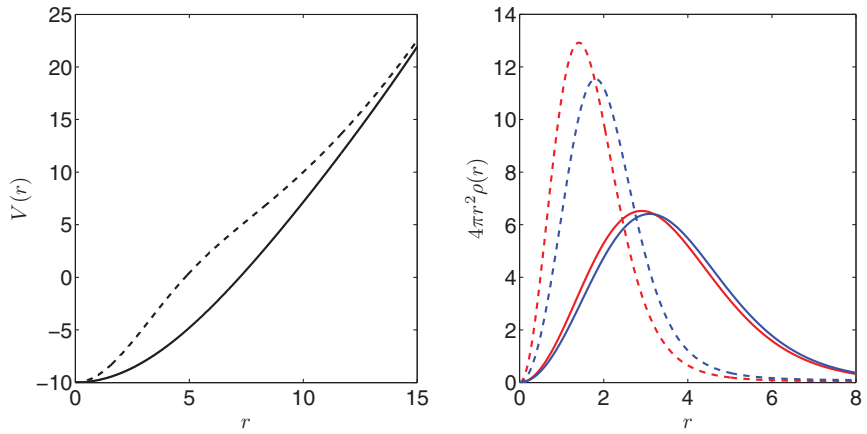

FIG. 9. Left plot shows the external potential for both species of soft particles at $t = 0$ (solid line) and $t > 0$ (dashed line). Right plot shows the initial (solid line) and final (dashed line) equilibrium particle distributions for the smaller species (red) and larger species (blue).

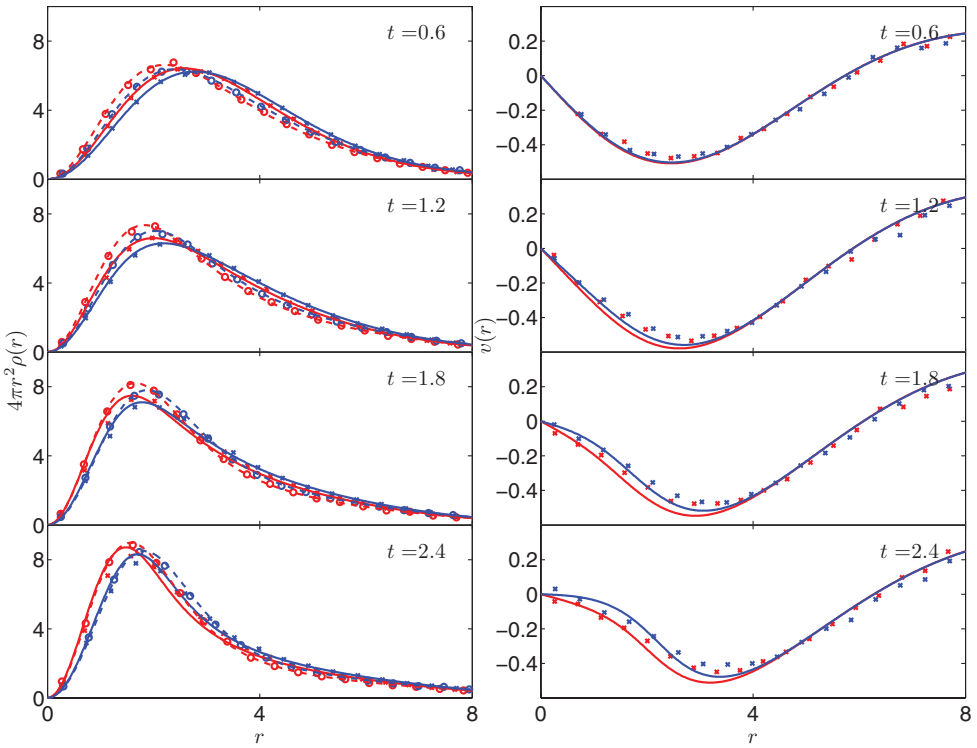

FIG. 10. Snapshots of radial particle distributions and velocities at various times for 25 particles of each species of soft particle. Species 1 in red and species 2 in blue. Lines show DDFT calculations, symbols stochastic dynamics for systems with (solid/crosses) and without (dashed/circles) inertia.

and the corresponding stochastic dynamics. However, the inclusion of inertia strongly modifies the dynamics, especially at early times.

IV. DISCUSSION

We have derived a general DDFT, including inertia and HI, for systems with an arbitrary number of species of colloidal particles. We have shown the very good qualitative and quantitative agreement between the DDFT and the full underlying Langevin dynamics for systems of 3D hard spheres in a spherically-symmetric external potential. We have also demonstrated the importance of including HI in multi-species systems, as well as an efficient and accurate numerical scheme based on spectral methods for integro-differential equations.

The derivation of the multi-species DDFT presented here requires three approximations. The first, the adiabatic approximation, is common to all DDFTs. However, it is an open problem to determine both the validity of this approximation and how to go beyond it. The second approximation is that of local equilibrium, which is again standard (and indeed also required by the analogous one-species phase space DDFTs[13,20,21]) but lacks in a systematic validation away from the high-friction limit. In particular, whilst it is formally possible to obtain a DDFT for molecular fluids by setting $\mathbf{\Gamma} = 0$, it is expected that this approximation breaks down in such a regime. In contrast to the adiabatic approximation, it is clear that one way in which to extend the formalism beyond this approximation is to consider higher momentum moments,[51] although this leads to significantly more complicated numerical schemes. Finally, we have implemented a two-body approximation to the HI terms, the extension of which is straightforward.

There are a number of promising extensions to the DDFT approach described here, including the effects of anisotropic particles, self-propelled particles, confined geometries, and external flows. Such extensions would allow the study of many systems of physical interest including cloud formation, wetting phenomena, and nanoparticle transport in the circulatory system. It is expected that both inertia and HI play important roles in the dynamics of these and many other related systems. In addition, we plan to extend our spectral-methods-based numerical implementation of DDFT to two dimensions, allowing the study of the effects of inertia and HI in a much wider range of systems.

ACKNOWLEDGMENTS

We acknowledge financial support from the European Research Council via Advanced Grant No. 247031, Imperial College through a DTG International Studentship, and the European Framework 7 via Grant No. 214919 (Multiflow). We are grateful to Dr. Nikos Savva and Mr. Peter Yatsyshin for stimulating discussions on DDFT and spectral methods.

[1] J. K. G. Dhont, *An Introduction to Dynamics of Colloids* (Elsevier, 1996).
[2] *Medical Applications of Colloids*, edited by E. Matijević (Springer, New York, 2008).
[3] D. F. Evans and H. Wennerström, *The Colloidal Domain: Where Physics, Chemistry, and Biology Meet* (Wiley, New York, 1999).
[4] H. Stone and S. Kim, AIChE J. **47**, 1250 (2001).
[5] F. Caruso, *Colloids and Colloid Assemblies: Synthesis, Modification, Organisation and Utilization of Colloid Particles* (Wiley, Weinheim, 2004).
[6] J. M. Brader, J. Phys.: Condens. Matter **22**, 363101 (2010).
[7] G. K.-L. Chan and R. Finken, Phys. Rev. Lett. **94**, 183001 (2005).
[8] R. Evans, Adv. Phys. **28**, 143 (1979).
[9] E. Roman and W. Dieterich, Phys. Rev. A **32**, 3726 (1985).
[10] J.-Z. Wu, AIChE J. **52**, 1169 (2006).
[11] J.-Z. Wu and Z.-D. Li, Annu. Rev. Phys. Chem. **58**, 85 (2007).
[12] M. Rex and H. Löwen, Eur. Phys. J. E **28**, 139 (2009).
[13] A. J. Archer, J. Chem. Phys. **130**, 014509 (2009).
[14] U. M. B. Marconi and P. Tarazona, J. Chem. Phys. **124**, 164901 (2006).
[15] U. M. B. Marconi and S. Melchionna, J. Chem. Phys. **126**, 184109 (2007).
[16] U. M. B. Marconi, P. Tarazona, and F. Cecconi, J. Chem. Phys. **126**, 164904 (2007).
[17] U. M. B. Marconi, P. Tarazona, F. Cecconi, and S. Melchionna, J. Phys. Condens. Matter **20**, 494233 (2008).
[18] P. Tarazona and U. M. B. Marconi, J. Chem. Phys. **128**, 164704 (2008).
[19] U. M. B. Marconi and P. Tarazona, J. Chem. Phys. **110**, 8032 (1999).
[20] B. D. Goddard, A. Nold, N. Savva, G. A. Pavliotis, and S. Kalliadasis, Phys. Rev. Lett. **109**, 120603 (2012).
[21] B. D. Goddard, A. Nold, N. Savva, P. Yatsyshin, and S. Kalliadasis, J. Phys.: Condens. Matter **25**, 035101 (2013).
[22] P. Yatsyshin, N. Savva, and S. Kalliadasis, J. Chem. Phys. **136**, 124113 (2012).
[23] A. Pereira and S. Kalliadasis, J. Fluid Mech. **692**, 53 (2012).
[24] N. Savva, S. Kalliadasis, and G. A. Pavliotis, Phys. Rev. Lett. **104**, 084501 (2010).
[25] E. Gavze and M. Shapiro, J. Fluid Mech. **371**, 59 (1998).
[26] H. R. Pruppacher, J. D. Klett, and P. K. Wang, *Microphysics of Clouds and Precipitation* (Taylor & Francis, 1998).
[27] H. Sigurgeirsson and A. M. Stuart, Phys. Fluids **14**, 4352 (2002).
[28] G. Falkovich, A. Fouxon, and M. Stepanov, Nature (London) **419**, 151 (2002).
[29] P. W. Longest and J. Xi, J. Aerosol Sci. **38**, 111 (2007).
[30] P. W. Longest and C. Kleinstreuer, J. Biomech. **36**, 421 (2003).
[31] A. J. Archer, J. Phys.: Condens. Matter **17**, 1405 (2005).
[32] A. J. Archer, J. Phys.: Condens. Matter **17**, S3253 (2005).
[33] R. Roth, M. Rauscher, and A. J. Archer, Phys. Rev. E **80**, 021409 (2009).
[34] K. Lichtner, A. J. Archer, and S. H. L. Klapp, J. Chem. Phys. **136**, 024502 (2012).
[35] A positive definite matrix M has an eigendecomposition $M = U^{-1}DU$ with U a unitary matrix and D a diagonal matrix with entries d_j. The square root of M is defined as $M^{1/2} = U^{-1}D^{1/2}U$, with $D^{1/2}$ the diagonal matrix with entries $d_j^{1/2}$.
[36] E. Runge and E. K. U. Gross, Phys. Rev. Lett. **52**, 997 (1984).
[37] Y. Rosenfeld, Phys. Rev. Lett. **63**, 980 (1989).
[38] R. Roth, R. Evans, A. Lang, and G. Kahl, J. Phys. Condens. Matter **14**, 12063 (2002).
[39] R. Roth, J. Phys.: Condens. Matter **22**, 063102 (2010).
[40] C. N. Likos, A. Lang, M. Watzlawek, and H. Löwen, Phys. Rev. E **63**, 031206 (2001).
[41] J. F. Lutsko, Adv. Chem. Phys. **144**, 1 (2010).
[42] D. J. Jeffrey and Y. Onishi, J. Fluid Mech. **139**, 261 (1984).
[43] U. M. B. Marconi and S. Melchionna, J. Chem. Phys. **131**, 014105 (2009).
[44] S.-L. Zhao and J. Wu, J. Chem. Phys. **134**, 054514 (2011).
[45] B. D. Goddard, G. A. Pavliotis, and S. Kalliadasis, Multiscale Model. Sim. **10**, 633 (2012).
[46] J. Rotne and S. Prager, J. Chem. Phys. **50**, 4831 (1969).
[47] P. E. Kloeden and E. Platen, *Numerical Solution of Stochastic Differential Equations* (Springer-Verlag, Berlin, 1992).
[48] R. M. Neal, Ann. Stat. **31**, 705 (2003).
[49] J. P. Boyd, *Chebyshev and Fourier Spectral Methods* (Dover, UK, 2001).
[50] E. Hairer and G. Wanner, *Solving Ordinary Differential Equations II. Stiff and Differential-Algebraic Problems*, Springer Series in Computational Mathematics Vol. 14 (Springer-Verlag, Berlin, 2006).
[51] K. H. Hughes and I. Burghardt, J. Chem. Phys. **136**, 214109 (2012).